

Photocatalytic degradation of contaminants of concern with composite NF-TiO₂ films under visible and solar light

H. Barndök · M. Peláez · C. Han · W. E. Platten III ·
P. Campo · D. Hermosilla · A. Blanco · D. D. Dionysiou

Received: 20 November 2012 / Accepted: 4 February 2013 / Published online: 24 February 2013
© Springer-Verlag Berlin Heidelberg 2013

Abstract This study reports the synthesis and characterization of composite nitrogen and fluorine co-doped titanium dioxide (NF-TiO₂) for the removal of contaminants of concern in wastewater under visible and solar light. Monodisperse anatase TiO₂ nanoparticles of different sizes and Evonik P25 were assembled to immobilized NF-TiO₂ by direct incorporation into the sol–gel or by the layer-by-layer technique. The composite films were characterized with X-ray diffraction, high-resolution transmission electron

microscopy, environmental scanning electron microscopy, and porosimetry analysis. The photocatalytic degradation of atrazine, carbamazepine, and caffeine was evaluated in a synthetic water solution and in an effluent from a hybrid biological concentrator reactor (BCR). Minor aggregation and improved distribution of monodisperse titania particles was obtained with NF-TiO₂-monodisperse (10 and 50 nm) from the layer-by-layer technique than with NF-TiO₂+monodisperse TiO₂ (300 nm) directly incorporated into the sol. The photocatalysts synthesized with the layer-by-layer method achieved significantly higher degradation rates in contrast with NF-TiO₂-monodisperse titania (300 nm) and slightly faster values when compared with NF-TiO₂-P25. Using NF-TiO₂ layer-by-layer with monodisperse TiO₂ (50 nm) under solar light irradiation, the respective degradation rates in synthetic water and BCR effluent were 14.6 and 9.5×10⁻³ min⁻¹ for caffeine, 12.5 and 9.0×10⁻³ min⁻¹ for carbamazepine, and 10.9 and 5.8×10⁻³ min⁻¹ for atrazine. These results suggest that the layer-by-layer technique is a promising method for the synthesis of composite TiO₂-based films compared to the direct addition of nanoparticles into the sol.

Responsible editor: Philippe Garrigues

H. Barndök · D. Hermosilla · A. Blanco
Department of Chemical Engineering,
Complutense University of Madrid, Avda. Complutense, s/n,
28040 Madrid, Spain

H. Barndök
e-mail: hbarndok@quim.ucm.es

D. Hermosilla
e-mail: dhermosilla@quim.ucm.es

A. Blanco
e-mail: ablanco@quim.ucm.es

M. Peláez · C. Han · W. E. Platten III · P. Campo · D. D. Dionysiou
Environmental Engineering and Science Program,
University of Cincinnati, Cincinnati, OH, USA

M. Peláez
e-mail: pelaezma@mail.uc.edu

C. Han
e-mail: hanck@mail.uc.edu

W. E. Platten III
e-mail: plattewe@mail.uc.edu

P. Campo
e-mail: campomp@ucmail.uc.edu

D. D. Dionysiou (✉)
Nireas-International Water Research Centre,
University of Cyprus, 20537 Nicosia, Cyprus
e-mail: dionysios.d.dionysiou@uc.edu

Keywords NF-TiO₂ · Monodisperse · Sol–gel method · Carbamazepine · Atrazine · Caffeine · TiO₂ photocatalysis · Solar · Visible light · Contaminants · Emerging · Concern · Water · Reuse

Introduction

Contaminants of concern (COCs), especially pharmaceuticals and pesticides, are routinely detected in the effluents of municipal wastewater treatment plants (WTPs), which presents a risk for the environment and human health

(Andreozzi et al. 2003; Belgiorno et al. 2007; Bernabeu et al. 2011; Castiglioni et al. 2006; Glassmeyer et al. 2005; Ho et al. 2011; Joss et al. 2005). Carbamazepine (CMP), a widely used anticonvulsant and mood-stabilizing drug (WHO 2002), is frequently identified downstream of sewage treatment plants in several European countries (Andreozzi et al. 2003; Bernabeu et al. 2011; Castiglioni et al. 2006; Joss et al. 2005) as well as in the USA (Glassmeyer et al. 2005). Likewise, atrazine (ATR) is a commonly found herbicide in WTP effluents around the USA (Glassmeyer et al. 2005; USEPA 2003) and Australia (Ho et al. 2011). According to the U.S. Environmental Protection Agency, ATR has a suspected impact on gonadal development in amphibians. Moreover, the European Union (EU) considers it an endocrine disruptor and, therefore, a priority substance in the EU Water Framework Directive 2008/105/EC (EC 2008). The treatment of these compounds by conventional biological methods, such as activated sludge process, trickling filter, membrane bioreactor, and suspended-biofilm reactor, achieves only partial removal of these chemicals (Andreozzi et al. 2003; Belgiorno et al. 2007; Bernabeu et al. 2011; Castiglioni et al. 2006; Glassmeyer et al. 2005; Ho et al. 2011; Joss et al. 2005). For this reason, the integrated use of advanced oxidation processes (AOPs) with biological treatment is of great interest as they have shown the capability to polish effluent streams containing biorefractory organics (Andreozzi et al. 2003; Belgiorno et al. 2007; Bernabeu et al. 2011; Rizzo et al. 2009). Titanium dioxide (TiO₂)-based nanotechnology has gained recognition as a promising AOP for water remediation due to the process high decomposition efficiency and TiO₂ green characteristics, e.g., low toxicity, inert nature, and relatively low cost (Antonioni et al. 2008; Choi et al. 2007; Fujishima et al. 2000). This non-selective treatment even degrades trace level concentrations that are difficult or expensive to remove with conventional methods (Balasubramanian et al. 2004; Lin et al. 2006).

Photocatalytic degradation employing TiO₂-based nanomaterials in slurry suspension or colloidal solution has been carried out successfully for both ATR (Hincapie et al. 2005; Li et al. 2012; Mourao et al. 2010; Parra et al. 2004) and CMP (Bernabeu et al. 2011; Chong and Jin 2012; Doll and Frimmel 2004; Laera et al. 2011). However, TiO₂ immobilization to avoid a filtration step could appreciably improve the cost-effectiveness of the operation (Balasubramanian et al. 2004; Goetz et al. 2009; Han et al. 2011; Miranda-Garcia et al. 2011; Pelaez et al. 2010). Hence, among current challenges of the TiO₂-based nanotechnology for environmental applications include enhancement of the structural and the photocatalytic properties of the immobilized catalysts.

Satisfactory removals of ATR, as a sole contaminant in synthetic solutions, have been achieved with TiO₂ immobilized on a supporting media under UV or solar

light irradiation (Goetz et al. 2009; McMurray et al. 2006; Parra et al. 2004). However, COCs are usually not the only substances present in effluents, so their photocatalytic degradation may be hampered by the presence of other organic and inorganic constituents that exert a stronger selectivity towards the catalyst or the oxidant species (Chong et al. 2011; Klamerth et al. 2009; Laera et al. 2011). Very few papers deal with supported photocatalysts for the treatment of COCs in mixtures. Miranda-Garcia et al. (2011) studied the degradation of 15 COCs in simulated and real municipal wastewater with TiO₂ immobilized on glass spheres under solar irradiation. ATR and CMP demonstrated to be the most recalcitrant since they presented the lowest degradation rates among the studied compounds.

The UV-restricted photoactivation of TiO₂ limits the utilization of a higher portion of the solar spectrum (i.e., visible light) to generate reactive oxidizing species. Several approaches, including metal and non-metal doping, dye-sensitization, and coupled semiconductors, have been applied to overcome this 3.2-eV band gap energy (Pelaez et al. 2012b). For drinking water treatment, non-metallic dopants (e.g., nitrogen, sulfur, fluorine, or carbon) are preferable because these elements do not show leakage as metals or other semiconductors do (Asahi et al. 2001; Choi et al. 2007; Lin et al. 2006; Rengifo-Herrera et al. 2009; Subagio et al. 2010). Nitrogen and fluorine codoped TiO₂ (NF-TiO₂) films with enhanced structural properties have been synthesized using a modified sol-gel procedure and successfully applied to the photocatalytic degradation of cyanobacterial toxins in water (Pelaez et al. 2009; Pelaez et al. 2010). Additionally, the incorporation of Evonik® P25-TiO₂ nanoparticles into the sol-gel improved the physicochemical and optical properties of the TiO₂ film (Chen and Dionysiou 2008; Pelaez et al. 2011). Therefore, studying the effect of different nanoparticles added into the NF-TiO₂ sol-gel to improve its photocatalytic efficiency is of great interest.

In this work, monodisperse anatase TiO₂ nanoparticles of various particle sizes (Han et al. 2012) were assembled to the immobilized NF-TiO₂ films by direct incorporation into the NF-TiO₂ sol-gel or by employing the layer-by-layer technique. The performance of these composite films in the degradation of a mixture of COCs in both synthetic water and wastewater was evaluated under visible and solar irradiation, and compared with the performance of NF-TiO₂-P25. The tested COCs were CMP and ATR as the representatives of the most persistent pharmaceuticals and pesticides typically present in WTP effluents. In addition, caffeine (CAF) was included as one of the most commonly detected contaminants in wastewater streams worldwide (Bernabeu et al. 2011; Glassmeyer et al. 2005; Kolpin et al. 2002).

Materials and methods

Reagents and sample preparation

ATR, CAF, and CMP were obtained from Sigma-Aldrich (USA). NF-TiO₂ was prepared using a modified sol–gel method reported by Pelaez et al. (2010). Briefly, a fluorsurfactant (Zonyl FS 300, Fluka), which served as a pore template and fluorine dopant, was dissolved in isopropyl alcohol (Fisher, USA). After the addition of glacial acetic acid (Fisher, USA), ethylenediamine (Fisher, USA) was added as a nitrogen precursor. Titanium tetraisopropoxide (TTIP; Sigma-Aldrich, USA, 97 %) was added dropwise to the sol, followed by additional acetic acid for peptidization. Monodisperse anatase titania was synthesized by a sol–gel method described by Han et al. (2012). In brief, CaCl₂ solutions of varying concentrations (to provide different ionic strength for the particle size control) were added to methanol (Tedia, USA). After mixing, TTIP was added dropwise as the titanium precursor.

Two different ways of incorporating the nanoparticles into the composite NF-TiO₂ films were implemented. In the first method, Evonik® P25-TiO₂ or monodisperse titania nanoparticles (300 nm) were incorporated directly into the NF-TiO₂ sol–gel at 5 gL⁻¹ and sonicated. Subsequently, the sol was deposited on the substrate by dip-coating and immobilized as described elsewhere (Pelaez et al. 2012a). The second approach consisted in a layer-by-layer technique employing a separate solution of monodisperse titania with a particle size of 10 or 50 nm. The first coating consisted of a NF-TiO₂ film followed by monodisperse titania one. This process of merging NF-TiO₂ with monodisperse titania on top of it was repeated three times layer-by-layer until a final layer of monodisperse titania was achieved (six layers in total). The procedure of immobilization of the composite films is described elsewhere (Pelaez et al. 2012a).

Characterization of the films

A Tristar 3000 (Micromeritics) porosimeter analyzer was employed for the determination of BET surface area, pore volume, porosity, and BJH pore size distribution of the composite NF-TiO₂ films. The films were scraped, and the samples were collected as powder and purged with N₂ for 2 h at 150 °C using Flow prep 060 (Micromeritics). The film morphology was characterized with an environmental scanning electron microscope (ESEM, Philips XL 30 ESEM-FEG). The crystallographic structure of the synthesized TiO₂ films was determined with a X'Pert PRO (Philips) XRD diffractometer with Cu Kα (λ=1.5406 Å) radiation. Optoelectronic properties were derived from diffuse reflectance

spectra obtained on a UV–vis spectrophotometer (Shimadzu 2501 PC) equipped with an integrated sphere attachment (ISR 1200) with BaSO₄ reference standard.

Photocatalytic experiments

The photocatalytic degradation of ATR, CAF, and CMP was carried out both in a synthetic water solution (MilliQ-grade water) and in the effluent of a hybrid biomass concentrator reactor (BCR; Scott 2012), which treated a medium strength synthetic municipal wastewater (see Table 3 for effluent characteristics prior to spiking). Stock solutions of the analytes were prepared in MilliQ-grade water, and all the analytes were added together in aforementioned matrices at 4 μmolL⁻¹. A borosilicate glass vessel reactor (i.d. 4.7 cm) containing 10 mL of spiked solution (0.58 cm of aqueous irradiated layer) and a composite film was sealed with parafilm and cooled down with a fan to prevent evaporation. The solution was irradiated with a 500-W solar simulator (Newport Corporation) equipped with AM 1.5 and infrared filters. The light intensity was 70 Wcm⁻² and was measured with a radiant power meter (Newport Corporation). When the experiments were performed in the visible range (420–700 nm), the measured light intensity was 40 Wcm⁻². The experiments were carried out in duplicates.

The COCs were analyzed by liquid chromatography–electrospray ionization–tandem mass spectrometry with a 1200 Series rapid resolution liquid chromatograph and 6410A triple quadrupole mass spectrometer equipped with a G1948B electrospray ionization source (Agilent, Palo Alto, CA, USA). The ESI was operated in positive mode. The analytes were separated with a Zorbax Eclipse XDB-C18 (2.1 × 50 mm, 3.5 μm) column (Agilent, Palo Alto, CA, USA). The flow was 0.5 mL/min. The mobile phase was comprised of water (A) and methanol (B), both containing ammonium formate (5 mM). At time 0, the eluent composition was 90 % (A) and 10 % (B), being 36 % (A) and 64 % (B) after 12 min. The analytes were detected in the following selected reactions: ATR *m/z* 216 → *m/z* 174, CAF *m/z* 195 → *m/z* 138, and CMP *m/z* 237 → *m/z* 194.

Results and discussion

Morphology and microstructure of the composite NF-TiO₂ films

The overall surface morphology of the NF-TiO₂ composite materials was examined by ESEM. Rough and porous surfaces were observed in all of the studied composite films (Figs. 1 and 2). The high surface roughness is a characteristic of NF-TiO₂ films synthesized with the abovementioned sol–gel method. Nevertheless, a rougher surface could

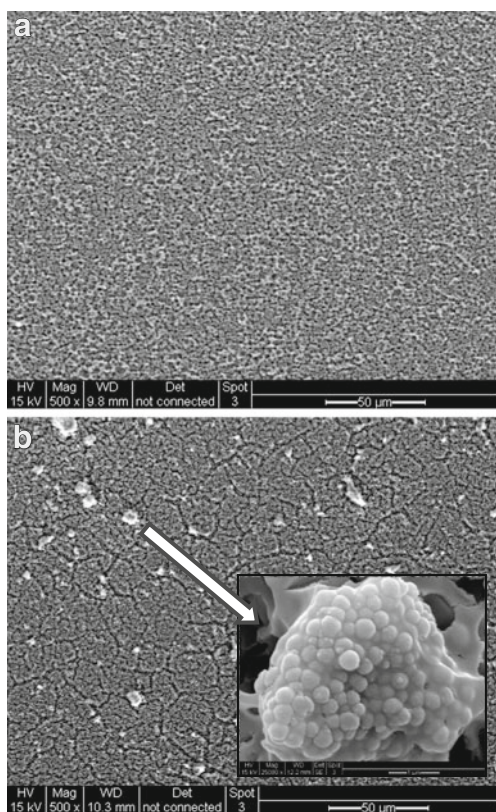


Fig. 1 ESEM images of **a** NF-TiO₂-P25, **b** NF-TiO₂+monodisperse titania (300 nm) added directly to the sol

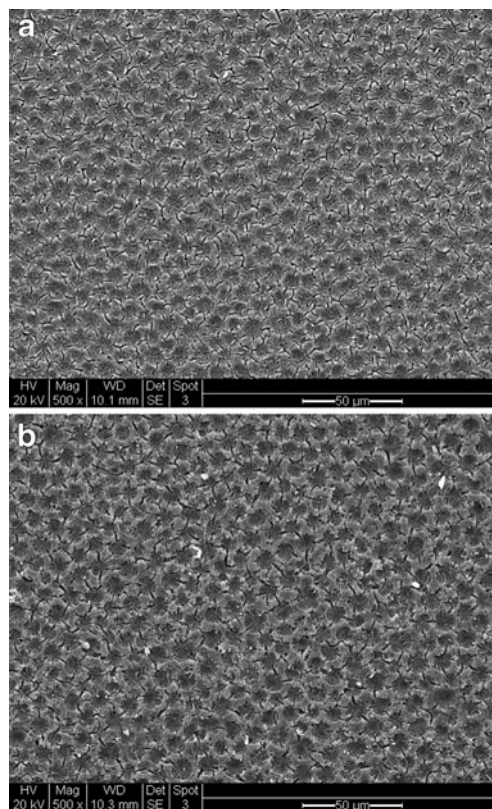


Fig. 2 ESEM images of the catalysts from the layer-by-layer method: **a** NF-TiO₂-monodisperse TiO₂ (50 nm). **b** NF-TiO₂-monodisperse TiO₂ (10 nm)

provide a larger surface area for the photocatalytic reactions and more effective light absorbance than smoother surfaces (Pelaez et al. 2010; Provata et al. 1998). Based on Figs. 1 and 2, the difference among films was mainly due to the surface coverage. Higher surface coverage and more uniform distribution of nanoparticle additives were achieved in those films composed with P25 (Fig. 1a) than with the composite film containing monodisperse nanoparticles of 300 nm (Fig. 1b). In the latter, the surface coverage was greatly decreased due to the extensive aggregation of nanoparticles. Although the presence of aggregates was observed in all the catalysts cases (Figs. 1 and 2), much larger nanoparticle clusters were formed when monodisperse anatase titania was directly added into the sol-gel (Fig. 1b). Nevertheless, with the layer-by-layer technique, when the initially fairly well-distributed sol of the monodisperse TiO₂ was deposited as an even layer on top of the NF-TiO₂ by dip-coating, fewer aggregates and improved distribution of monodisperse titania was obtained (Fig. 2). It can be concluded that the dispersion of the monodisperse particles is higher when employing the layer-by-layer method than when added directly into the NF-TiO₂ sol in a powdered form after recovering the monodisperse particles from the initial solution. The smaller particle size (50 and 10 nm) could probably also enhance the distribution of monodisperse titania. However, no notable difference was found in the ESEM

images when using the particle size of 50 nm (Fig. 2a) or 10 nm (Fig. 2b), showing that the uniformity of the distribution of monodisperse particles is similar in the size range of 10 to 50 nm. Since the COCs degradation preferentially occurs on the catalyst surface, a higher interaction is expected with the film that has the highest surface area coverage (Linsebigler et al. 1995). Therefore, since fewer aggregates and improved

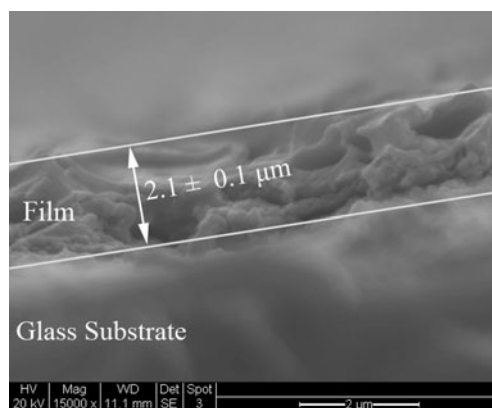


Fig. 3 Cross-section ESEM image of the film thickness of the composite NF-TiO₂ with monodisperse TiO₂ by the layer-by-layer technique

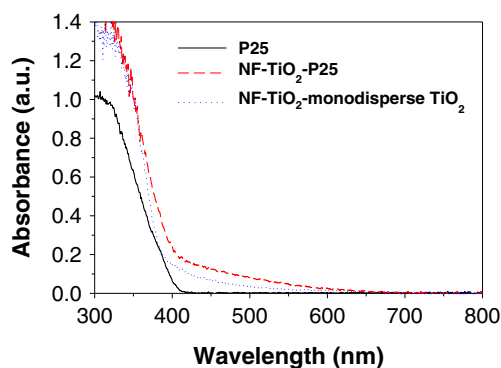


Fig. 4 Absorbance spectra of P25, composite NF-TiO₂-P25, and NF-TiO₂-monodisperse TiO₂

distribution of monodisperse titania were obtained by the layer-by-layer method, improved degradation similar to, or higher than, the NF-TiO₂-P25 could be expected.

In spite of the doubled number of layers, the films prepared by the layer-by-layer method had a slightly lower film thickness (Fig. 3) than the composite NF-TiO₂-P25 (Pelaez et al. 2012a) where nanoparticle additives were incorporated directly into the sol. This, however, did not lead to lower photocatalytic activity for the NF-TiO₂-monodisperse compared to NF-TiO₂-P25 (see “Photocatalytic evaluation of the composite NF-TiO₂ films synthesized layer-by-layer with the monodisperse TiO₂” section).

According to XRD analysis, NF-TiO₂-P25 films exhibited two crystal phases, anatase and rutile (confirming the presence of P25 nanoparticles). On the other hand, anatase was the only form detected for NF-TiO₂-monodisperse (300 nm) and NF-TiO₂ layer-by-layer with monodisperse TiO₂ (10 and 50 nm). Dopant-related crystal phases were not observed since the amount of nitrogen and fluorine does not produce significant changes in the TiO₂ structure (Pelaez et al. 2010).

The absorbance spectra of the Evonik P25, the composite NF-TiO₂-P25, and the NF-TiO₂-monodisperse TiO₂ are shown in Fig. 4. While the reference sample of P25 showed no absorption towards visible light, the composite NF-TiO₂ exhibited absorption spectra extended to the visible range of 400–500 nm to a small degree. This is due to the N and F doping, whereas the P25 and monodisperse titania additives

most likely reduce the visible light absorption capacity of the NF-TiO₂ (Pelaez et al. 2012a).

Porosimetry analysis was carried out for further characterization of the films. Table 1 summarizes the structural characteristics of all the composite NF-TiO₂ films. The BET surface area increased with the direct addition of monodisperse titania (300 nm) into the NF-TiO₂ sol, compared to the NF-TiO₂-P25 composite film. The formation of different aggregate sizes due to the specific properties of the monodisperse titania and P25 can lead to the different values of BET area obtained. The films with monodisperse titania added by the layer-by-layer method presented BET surface area similar to or even smaller than the NF-TiO₂-P25 (monodisperse titania of 50 and 10 nm, respectively). The smaller monodisperse particles of 10 nm could smoothen the surface roughness of the TiO₂ film, but doing so also decreases the available surface area. Fairly similar pore size distribution was observed in all studied composite films.

Photocatalytic evaluation of the composite films

The photocatalytic degradation of the studied COCs followed pseudo-first-order kinetics. Regardless of the catalyst used or the aqueous matrix, CAF presented the highest degradation rate followed by CMP and ATR (see Table 2). ATR seemed to be more resistant at the early stages of the photocatalytic reaction (see Figs. 5, 6, 7, and 8), probably because of the higher persistence of ATR due to its chemical structure and/or because of the competitive adsorption on the catalyst surface by the other compounds in the mixture (Zahraa et al. 2003). However, the final concentrations of all the compounds were not substantially different after 7 h of degradation, which shows the high efficiency of the treatment under the experimental conditions.

Photocatalytic evaluation of the composite films with nanoparticle additives directly incorporated to the NF-TiO₂ sol

Preliminary studies were carried out in synthetic water, comparing the two composite catalysts with nanoparticle additives directly incorporated into the NF-TiO₂ sol both

Table 1 Structural characteristics of NF-TiO₂ films with different nanoparticle additives

Material	S _{BET} (m ² g ⁻¹)	Pore volume (cm ³ g ⁻¹)	Porosity (%)	Crystal phase
NF-TiO ₂ -monodisperse (50 nm) ^a	110.6	0.189	42.4	Anatase
NF-TiO ₂ -monodisperse (10 nm) ^a	99.4	0.173	40.3	Anatase
NF-TiO ₂ -P25	111.5	0.154	37.5	Anatase/Rutile
NF-TiO ₂ -monodisperse (300 nm) ^b	147.7	0.189	42.5	Anatase

^a Monodisperse titania incorporated by the layer-by-layer method

^b Monodisperse titania added directly to the sol-gel

under visible and solar light (Fig. 5). Limited visible light degradation of all COCs was observed with NF-TiO₂-P25 and NF-TiO₂+monodisperse titania (300 nm), indicating the persistence of the COCs under the conditions tested.

Nevertheless, the COCs were effectively degraded under solar light with both composite films in synthetic solution. Higher degradation efficiency in terms of higher kinetic constant *k* (minutes; Table 2) was obtained with NF-TiO₂-P25 (see Fig. 5a) when compared with NF-TiO₂+monodisperse titania (300 nm; Fig. 5b). ATR had the lowest reaction kinetics, the *k* values in the case of using P25 additive or monodisperse TiO₂ (300 nm) were 8.8 and 2.5 × 10⁻³ min⁻¹, respectively (Table 2). In terms of removal, after 2 h of solar light irradiation, 77 % of CAF, 72 % of CMP, and 56 % of ATR were degraded by NF-TiO₂-P25, while with NF-TiO₂+monodisperse titania of 300 nm, the percentages were 54, 50, and 24 %, respectively.

The degradation of COCs was slower in the BCR effluent than in the synthetic water solution (Fig. 6). With NF-TiO₂-P25, the *k* value for the CMP degradation in synthetic water (12.6 × 10⁻³ min⁻¹) decreased to 8.4 × 10⁻³ min⁻¹ (by about 30 %; see Table 2). This decrease of degradation rates compared to the synthetic water is explained by the fact that the BCR effluent is a complex matrix containing several inorganic constituents that may compete with the analytes during the photocatalytic process (Table 3). The presence of SO₄²⁻ and Cl⁻ (316 and 59 mgL⁻¹, respectively) and a total alkalinity of 156 mgL⁻¹ (usually caused by the bicarbonates in great extent) were most likely the reason for the decrease in the degradation rates. Those inorganic species are reported to inhibit the TiO₂ photocatalysis, principally as competitors for the adsorption on the catalyst surface or as the scavengers of •OH radical (Burns et al. 1999; Yalap and Balcioglu 2009). Furthermore, the higher pH of the BCR effluent (7.9) compared to the synthetic solution at 5.7 could also affect the

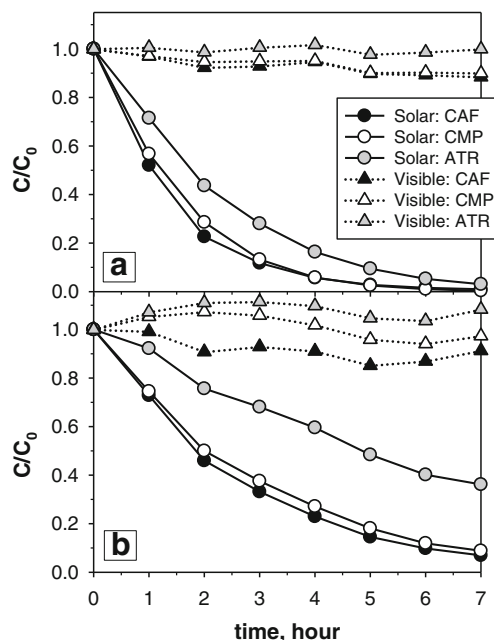


Fig. 5 Photocatalytic degradation of COCs in synthetic solution under visible and solar irradiation by **a** NF-TiO₂-P25, **b** NF-TiO₂+monodisperse titania (300 nm) added directly to the sol

photocatalytic reactions (Barndök et al. 2012). As the surface of NF-TiO₂ is negatively charged at pH values above ~6.0 as well as CMP (Achilleos et al. 2010; Pelaez et al. 2009), the adsorption of the compound on the surface of the catalyst is hindered by the action of repulsive electrostatic forces.

The negative effect of the BCR effluent on the degradation was even greater when monodisperse TiO₂ (300 nm) was directly incorporated to the sol (Table 2). For CAF, that exhibited the highest degradation kinetics in both water matrices, the *k* values in the synthetic water decreased in the BCR effluent by about 20 % when using P25 additive, but more than 50 % when employing TiO₂ (300 nm). In terms of

Table 2 First-order kinetic constants of the photocatalytic degradation of COCs under solar light irradiation in (a) synthetic solution and (b) BCR effluent

Catalyst	NF-TiO ₂ -monodisperse(50 nm) ^a			NF-TiO ₂ -monodisperse (10 nm) ^b			NF-TiO ₂ -P25			NF-TiO ₂ -monodisperse (300 nm) ^b			
	Compound	<i>t</i> _{1/2} min	<i>k</i> ·10 ³ min ⁻¹	<i>R</i> ²	<i>t</i> _{1/2} min	<i>k</i> ·10 ³ min ⁻¹	<i>R</i> ²	<i>t</i> _{1/2} min	<i>k</i> ·10 ³ min ⁻¹	<i>R</i> ²	<i>t</i> _{1/2} min	<i>k</i> ·10 ³ min ⁻¹	<i>R</i> ²
Synthetic solution													
CAF		47.4	14.6	1.00	54.8	12.6	1.00	60.9	11.4	0.99	105.7	6.56	1.00
CMP		55.5	12.5	0.99	59.1	11.7	1.00	55.1	12.6	0.99	116.9	5.93	1.00
ATR		63.6	10.9	1.00	70.2	9.9	0.99	78.7	8.8	0.97	275.4	2.52	0.99
BCR effluent													
CAF		72.8	9.52	1.00	70.8	9.79	1.00	76.1	9.11	0.99	199.4	3.48	1.00
CMP		77.3	8.97	0.95	79.4	8.73	0.93	82.4	8.42	0.99	245.2	2.83	0.99
ATR		118.8	5.83	0.99	104.8	6.61	0.99	134.2	5.17	0.99	685.2	1.01	1.00

^a Monodisperse titania incorporated by the layer-by-layer method

^b Monodisperse titania added directly to the sol-gel

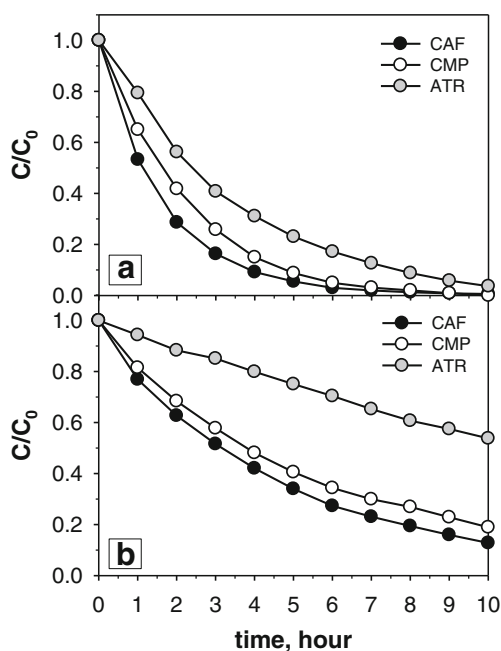


Fig. 6 Photocatalytic degradation of COCs in BCR effluent under solar light employing **a** NF-TiO₂-P25, **b** NF-TiO₂+monodisperse titania (300 nm) added directly to the sol

removal efficiency, after 2 h of degradation, 71 % of CAF, 59 % of CMP, and 44 % of ATR were removed with NF-TiO₂-P25 (Fig. 6a); however, with NF-TiO₂+monodisperse TiO₂ (300 nm), the removal percentages were only 37, 32, and 12 % for CAF, CMP, and ATR, respectively (Fig. 6b). The superior

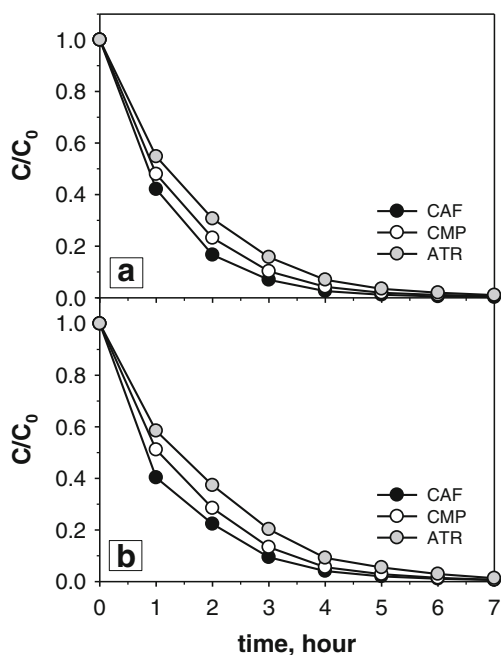


Fig. 7 Photocatalytic degradation of COCs in synthetic solution under solar irradiation by catalysts from the layer-by-layer method: **a** NF-TiO₂-monodisperse TiO₂ (50 nm), **b** NF-TiO₂-monodisperse TiO₂ (10 nm)

Table 3 Characterization of the BCR effluent

Effluent characteristic	Measure	Unit
pH	7.9	
Total alkalinity	156	mgL ⁻¹
Total hardness	64	mgL ⁻¹
Turbidity	0.13	NTU
Conductivity	1,055	μS
COD	<3	mgL ⁻¹
TOC	4.1	mgL ⁻¹
Cl ⁻	59	mgL ⁻¹
NO ₃ ⁻	14	mgL ⁻¹
PO ₄ ³⁻	2.8	mgL ⁻¹
SO ₄ ²⁻	316	mgL ⁻¹

photocatalytic performance by NF-TiO₂-P25 compared to NF-TiO₂+monodisperse titania (300 nm) was mainly due to the different properties of the material. Although the composite film containing monodisperse nanoparticles of 300 nm presented a higher surface area than those prepared with P25 (Table 1), a higher surface coverage was achieved in the film composed with P25 (Fig. 1a). The more uniform dispersion of P25 was a reason for the better photocatalytic activity of NF-TiO₂-P25, while the highly aggregated monodisperse particles brought along poor surface area coverage and, thus, inferior photocatalytic efficiency. Such lower activity in photocatalytic degradation was accentuated in the more complex nature of the BCR effluent.

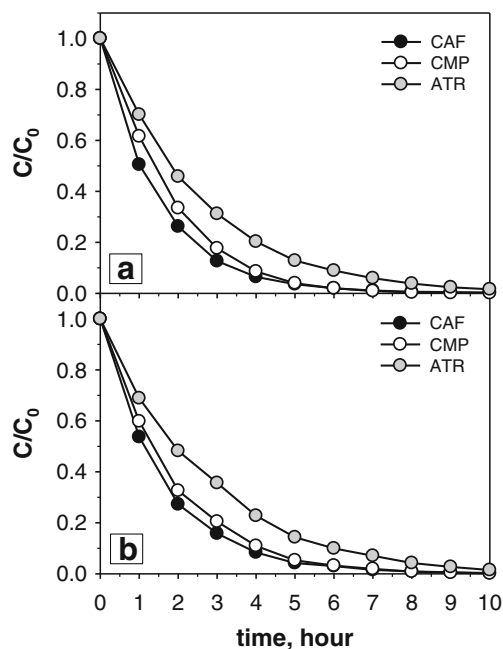


Fig. 8 Photocatalytic degradation of COCs in BCR effluent under solar light employing catalysts from the layer-by-layer method: **a** NF-TiO₂-monodisperse TiO₂ (50 nm), **b** NF-TiO₂-monodisperse TiO₂ (10 nm)

Photocatalytic evaluation of the composite NF-TiO₂ films synthesized layer-by-layer with the monodisperse TiO₂

The catalysts synthesized with the layer-by-layer method achieved higher degradation rates than those where nanoparticle additives were directly incorporated into the NF-TiO₂ sol. As shown in Fig. 7, in the synthetic water solution, the photocatalysts comprising of monodisperse titania of 50 and 10 nm (Fig. 7a and b, respectively) yielded slightly higher degradation than NF-TiO₂-P25 (see Table 2). The k values for ATR were 10.9 and $9.9 \times 10^{-3} \text{ min}^{-1}$ using NF-TiO₂ layer-by-layer with monodisperse TiO₂ of 50 and 10 nm, respectively. In terms of removal, after 2-h period of exposure, 83 % of CAF, 77 % of CMP, and 69 % of ATR were removed when using monodisperse particles of 50 nm (Fig. 7a), and 78 % of CAF, 72 % of CMP, and 63 % of ATR were removed when using monodisperse particles of 10 nm (Fig. 7b).

With the catalysts from the layer-by-layer method, the degradation of COCs was also slower in the BCR effluent compared to the synthetic water solution (Table 2). With NF-TiO₂-monodisperse TiO₂ (10 nm), the k value for the COCs degradation was decreased by about $3 \times 10^{-3} \text{ min}^{-1}$ when compared with the kinetics in synthetic water. In terms of removal efficiency, after 2 h, 73 % of CAF, 67 % of CMP, and 52 % of ATR were removed when adding monodisperse particles of 10 nm by the layer-by-layer technique and 67 % of CAF, 68 % of CMP, and 48 % of ATR were removed using monodisperse particles of 50 nm (Fig. 8a, b). As witnessed in the characterization of the composite films (“Morphology and microstructure of the composite NF-TiO₂ films” section), the difference between the catalyst materials was mainly due to the surface area coverage. Based on the ESEM images (Fig. 2), there was no remarkable variation in the surface coverage between the films made by the layer-by-layer technique. In the 10- to 50-nm range, a change in size of the monodisperse particles did not induce a relevant modification in the distribution of nanoparticles and, thus, in the coverage of the merged catalyst surface. Hence, NF-TiO₂ films synthesized by the layer-by-layer method with monodisperse TiO₂ with either 10 or 50 nm of particle size possess similar photocatalytic activities.

Conclusions

The incorporation method of the monodisperse titania to NF-TiO₂ played a significant role in the final physicochemical and photocatalytic properties of the composite film. Fewer nanoparticle aggregates and improved distribution of monodisperse TiO₂ were obtained with the layer-by-layer technique compared to the direct addition of monodisperse particles into the sol. The COCs were effectively degraded under solar light with NF-TiO₂-monodisperse (10

and 50 nm size) from the layer-by-layer technique as well as with NF-TiO₂-P25, whereas monodisperse TiO₂ of 300 nm directly incorporated into the NF-TiO₂ sol only achieved partial COCs degradation. Due to the presence of several inorganic components and higher pH, slower degradation was observed in the BCR effluent than in the synthetic solution (k values decreased by about $3\text{--}4 \times 10^{-3} \text{ min}^{-1}$). NF-TiO₂-monodisperse (10 and 50 nm) presented the best performance in both aqueous matrices (in the first 2 h, about 80, 75, and 70 % removal in synthetic water and about 70, 70, and 50 % removal in the BCR effluent was obtained for CAF, CMP, and ATR, respectively). These results imply that the layer-by-layer technique is a promising technique for the synthesis of composite TiO₂-based films as opposed to the direct addition of nanoparticles into the prepared sol-gel, and further optimization of the method is warranted.

Acknowledgments This research was funded by the Cyprus Research Promotion Foundation through Desmi 2009–2010, which is co-funded by the Republic of Cyprus and the European Regional Development Fund of the EU (contract NEA IPODOMI/STRATH/0308/09); the Ministry of Science and Innovation of Spain (project “AGUA Y ENERGÍA”, CTM2008-06886-C02-01); the European Commission (project “AQUAFIT4USE”, 211534); and the Archimedes Foundation (Estonia), which is granting Helen Barndök’s Ph.D. studies.

References

- Achilleos A, Hapeshi E, Xekoukoulotakis NP, Mantzavinos D, Fatta-Kassinos D (2010) UV-A and solar photodegradation of ibuprofen and carbamazepine catalyzed by TiO₂. *Separ Sci Technol* 45(11):1564–1570. doi:10.1080/01496395.2010.487463
- Andreozzi R, Raffaele M, Nicklas P (2003) Pharmaceuticals in STP effluents and their solar photodegradation in aquatic environment. *Chemosphere* 50(10):1319–1330. doi:10.1016/s0045-6535(02)00769-5
- Antoniou MG, Shoemaker JA, De La Cruz AA, Dionysiou DD (2008) Unveiling new degradation intermediates/pathways from the photocatalytic degradation of microcystin-LR. *Environ Sci Technol* 42(23):8877–8883. doi:10.1021/es801637z
- Asahi R, Morikawa T, Ohwaki T, Aoki K, Taga Y (2001) Visible-light photocatalysis in nitrogen-doped titanium oxides. *Science* 293(5528):269–271. doi:10.1126/science.1061051
- Balasubramanian G, Dionysiou DD, Suidan MT, Baudin I, Audin B, Laine JM (2004) Evaluating the activities of immobilized TiO₂ powder films for the photocatalytic degradation of organic contaminants in water. *Appl Catal B-Environ* 47(2):73–84. doi:10.1016/j.apcatb.2003.04.002
- Barndök H, Hermosilla D, Cortijo L, Negro C, Blanco A (2012) Assessing the effect of inorganic anions on TiO₂-photocatalysis and ozone oxidation treatment efficiencies. *J Adv Oxid Technol* 15(1):125–132
- Belgiorno V, Rizzo L, Fatta D, Della Rocca C, Lofrano G, Nikolaou A, Naddeo V, Meric S (2007) Review on endocrine disrupting-emerging compounds in urban wastewater: occurrence and removal by photocatalysis and ultrasonic irradiation for wastewater reuse. *Desalination* 215(1–3):166–176. doi:10.1016/j.desal.2006.10.035
- Bernabeu A, Vercher RF, Santos-Juanes L, Simon PJ, Lardin C, Martinez MA, Vicente JA, Gonzalez R, Llosa C, Arques A, Amat AM (2011)

- Solar photocatalysis as a tertiary treatment to remove emerging pollutants from wastewater treatment plant effluents. *Catal Today* 161(1):235–240. doi:10.1016/j.cattod.2010.09.025
- Burns RA, Crittenden JC, Hand DW, Selzer VH, Sutter LL, Salman SR (1999) Effect of inorganic ions in heterogeneous photocatalysis of TCE. *J Environ Eng-Asce* 125(1):77–85. doi:10.1061/(asce)0733-9372(1999)125:1(77)
- Castiglioni S, Bagnati R, Fanelli R, Pomati F, Calamari D, Zuccato E (2006) Removal of pharmaceuticals in sewage treatment plants in Italy. *Environ Sci Technol* 40(1):357–363. doi:10.1021/es050991m
- Chen Y, Dionysiou DD (2008) Bimodal mesoporous TiO₂-P25 composite thick films with high photocatalytic activity and improved structural integrity. *Appl Catal B-Environ* 80(1–2):147–155. doi:10.1016/j.apcatb.2007.11.010
- Choi H, Antoniou MG, Pelaez M, De la Cruz AA, Shoemaker JA, Dionysiou DD (2007) Mesoporous nitrogen-doped TiO₂ for the photocatalytic destruction of the cyanobacterial toxin microcystin-LR under visible light irradiation. *Environ Sci Technol* 41(21):7530–7535. doi:10.1021/es0709122
- Chong MN, Jin B (2012) Photocatalytic treatment of high concentration carbamazepine in synthetic hospital wastewater. *J Hazard Mater* 199:135–142. doi:10.1016/j.jhazmat.2011.10.067
- Chong MN, Jin B, Laera G, Saint CP (2011) Evaluating the photodegradation of carbamazepine in a sequential batch photoreactor system: impacts of effluent organic matter and inorganic ions. *Chem Eng J* 174(2–3):595–602. doi:10.1016/j.cej.2011.09.065
- Doll TE, Frimmel FH (2004) Kinetic study of photocatalytic degradation of carbamazepine, clofibrac acid, iomeprol and iopromide assisted by different TiO₂ materials—determination of intermediates and reaction pathways. *Water Res* 38(4):955–964. doi:10.1016/j.watres.2003.11.009
- EC (2008) Directive 2008/105/EC of the European Parliament and of the Council on the environmental quality standards in the field of water policy, amending and subsequently repealing Council Directives 82/176/EEC, 83/513/EEC, 84/156/EEC, 84/491/EEC and amending Directive 2000/60/EC. *Official Journal L348*:84–97
- Fujishima A, Rao TN, Tryk DA (2000) Titanium dioxide photocatalysis. *J Photoch Photobio C* 1:1–21. doi:10.1016/S1389-5567(00)00002-2
- Glassmeyer ST, Furlong ET, Kolpin DW, Cahill JD, Zaugg SD, Werner SL, Meyer MT, Kryak DD (2005) Transport of chemical and microbial compounds from known wastewater discharges: potential for use as indicators of human fecal contamination. *Environ Sci Technol* 39(14):5157–5169. doi:10.1021/es048120k
- Goetz V, Cambon JP, Sacco D, Plantard G (2009) Modeling aqueous heterogeneous photocatalytic degradation of organic pollutants with immobilized TiO₂. *Chem Eng Process* 48(1):532–537. doi:10.1016/j.cep.2008.06.013
- Han C, Luque R, Dionysiou DD (2012) Facile preparation of controllable size monodisperse anatase titania nanoparticles. *Chem Commun* 48(13):1860–1862. doi:10.1039/c1cc16050h
- Han C, Pelaez M, Likodimos V, Kontos AG, Falaras P, O'Shea K, Dionysiou DD (2011) Innovative visible light-activated sulfur doped TiO₂ films for water treatment. *Appl Catal B-Environ* 107(1–2):77–87. doi:10.1016/j.apcatb.2011.06.039
- Hincapie M, Maldonado MI, Oller I, Gernjak W, Sanchez-Perez JA, Ballesteros MM, Malato S (2005) Solar photocatalytic degradation and detoxification of EU priority substances. *Catal Today* 101(3–4):203–210. doi:10.1016/j.cattod.2005.03.004
- Ho L, Grasset C, Hoefel D, Dixon MB, Leusch FDL, Newcombe G, Saint CP, Brookes JD (2011) Assessing granular media filtration for the removal of chemical contaminants from wastewater. *Water Res* 45(11):3461–3472. doi:10.1016/j.watres.2011.04.005
- Joss A, Keller E, Alder AC, Gobel A, McArdell CS, Ternes T, Siegrist H (2005) Removal of pharmaceuticals and fragrances in biological wastewater treatment. *Water Res* 39(14):3139–3152. doi:10.1016/j.watres.2005.05.031
- Klamerth N, Miranda N, Malato S, Agueera A, Fernandez-Alba AR, Maldonado MI, Coronado JM (2009) Degradation of emerging contaminants at low concentrations in MWTPs effluents with mild solar photo-Fenton and TiO₂. *Catal Today* 144(1–2):124–130. doi:10.1016/j.cattod.2009.01.024
- Kolpin DW, Furlong ET, Meyer MT, Thurman EM, Zaugg SD, Barber LB, Buxton HT (2002) Pharmaceuticals, hormones, and other organic wastewater contaminants in US streams, 1999–2000: a national reconnaissance. *Environ Sci Technol* 36(6):1202–1211. doi:10.1021/es011055j
- Laera G, Jin B, Zhu H, Lopez A (2011) Photocatalytic activity of TiO₂ nanofibers in simulated and real municipal effluents. *Catal Today* 161(1):147–152. doi:10.1016/j.cattod.2010.10.037
- Li K, Huang Y, Yan L, Dai Y, Xue K, Guo H, Huang Z, Xiong J (2012) Simulated sunlight photodegradation of aqueous atrazine and rhodamine B catalyzed by the ordered mesoporous graphenitetania/silica composite material. *Catal Commun* 18:16–20. doi:10.1016/j.catcom.2011.11.008
- Lin YM, Tseng YH, Huang JH, Chao CC, Chen CC, Wang I (2006) Photocatalytic activity for degradation of nitrogen oxides over visible light responsive titania-based photocatalysts. *Environ Sci Technol* 40(5):1616–1621. doi:10.1021/es051007p
- Linsebigler AL, Lu GQ, Yates JT (1995) Photocatalysis on TiO₂ surfaces—principles, mechanisms, and selected results. *Chem Rev* 95(3):735–758. doi:10.1021/cr00035a013
- McMurray TA, Dunlop PSM, Byrne JA (2006) The photocatalytic degradation of atrazine on nanoparticulate TiO₂ films. *J Photoch Photobio A* 182(1):43–51. doi:10.1016/j.jphotochem.2006.01.010
- Miranda-Garcia N, Suarez S, Sanchez B, Coronado JM, Malato S, Ignacio Maldonado M (2011) Photocatalytic degradation of emerging contaminants in municipal wastewater treatment plant effluents using immobilized TiO₂ in a solar pilot plant. *Appl Catal B-Environ* 103(3–4):294–301. doi:10.1016/j.apcatb.2011.01.030
- Mourao HAJL, Malagutti AR, Ribeiro C (2010) Synthesis of TiO₂-coated CoFe₂O₄ photocatalysts applied to the photodegradation of atrazine and rhodamine B in water. *Appl Catal A-Gen* 382(2):284–292. doi:10.1016/j.apcata.2010.05.007
- Parra S, Stanca SE, Guasaquillo I, Thampi KR (2004) Photocatalytic degradation of atrazine using suspended and supported TiO₂. *Appl Catal B-Environ* 51(2):107–116. doi:10.1016/j.apcatb.2004.01.021
- Pelaez M, de la Cruz AA, Stathatos E, Falaras P, Dionysiou DD (2009) Visible light-activated N-F-codoped TiO₂ nanoparticles for the photocatalytic degradation of microcystin-LR in water. *Catal Today* 144(1–2):19–25. doi:10.1016/j.cattod.2008.12.022
- Pelaez M, Falaras P, Kontos AG, de la Cruz AA, O'Shea K, Dunlop PSM, Byrne JA, Dionysiou DD (2012a) A comparative study on the removal of cylindrospermopsin and microcystins from water with NF-TiO₂-P25 composite films with visible and UV-vis light photocatalytic activity. *Appl Catal B-Environ* 121:30–39. doi:10.1016/j.apcatb.2012.03.010
- Pelaez M, Falaras P, Likodimos V, Kontos AG, de la Cruz AA, Dionysiou DD (2011) Novel NF-TiO₂-P25 composite photocatalyst for the removal of microcystins and cylindrospermopsin under visible and solar light. *Abstr Pap Am Chem S* 241 (41-IEC)
- Pelaez M, Falaras P, Likodimos V, Kontos AG, de la Cruz AA, O'Shea K, Dionysiou DD (2010) Synthesis, structural characterization and evaluation of sol-gel-based NF-TiO₂ films with visible light-photoactivation for the removal of microcystin-LR. *Appl Catal B-Environ* 99(3–4):378–387. doi:10.1016/j.apcatb.2010.06.017
- Pelaez M, Nolan NT, Pillai SC, Seery MK, Falaras P, Kontos AG, Dunlop PSM, Hamilton JWJ, Byrne JA, O'Shea K, Entezari MH, Dionysiou DD (2012b) A review on the visible light active titanium dioxide photocatalysts for environmental applications. *Appl Catal B: Environ* 125:331–349

- Provata A, Falaras P, Xagas A (1998) Fractal features of titanium oxide surfaces. *Chem Phys Lett* 297(5–6):484–490. doi:10.1016/s0009-2614(98)01127-0
- Rengifo-Herrera JA, Pierzchala K, Sienkiewicz A, Forro L, Kiwi J, Pulgarin C (2009) Abatement of organics and *Escherichia coli* by N, S co-doped TiO₂ under UV and visible light. Implications of the formation of singlet oxygen (¹O₂) under visible light. *Appl Catal B-Environ* 88(3–4):398–406. doi:10.1016/j.apcatb.2008.10.025
- Rizzo L, Meric S, Guida M, Kassinos D, Belgiorno V (2009) Heterogenous photocatalytic degradation kinetics and detoxification of an urban wastewater treatment plant effluent contaminated with pharmaceuticals. *Water Res* 43(16):4070–4078. doi:10.1016/j.watres.2009.06.046
- Scott D et al (2012) Biological nitrogen and carbon removal in a gravity flow biomass concentrator reactor for municipal sewage treatment. *Chemosphere*. doi:10.1016/j.chemosphere.2012.08.045
- Subagio DP, Srinivasan M, Lim M, Lim T-T (2010) Photocatalytic degradation of bisphenol-A by nitrogen-doped TiO₂ hollow sphere in a vis-LED photoreactor. *Appl Catal B-Environ* 95(3–4):414–422. doi:10.1016/j.apcatb.2010.01.021
- USEPA (2003) Interim Reregistration Eligibility Decision for Atrazine (Report of the United States Environmental Protection Agency). USEPA, Washington Case No. 0062
- WHO (2002) WHO model list of essential medicines. *World Health Organization Drug Information* 16(2):139–150
- Yalap KS, Balcioglu IA (2009) Effects of inorganic anions and humic acid on the photocatalytic and ozone oxidation of oxytetracycline in aqueous solution. *J Adv Oxid Technol* 12(1):134–143
- Zahraa O, Sauvanaud L, Hamard G, Bouchy M (2003) Kinetics of atrazine degradation by photocatalytic process in aqueous solution. *Int J Photoenergy* 5(2):87–93. doi:10.1155/s1110662x03000187